Supplementary Information for:

Combined mTORC1/mTORC2 Inhibition Blocks Growth and Induces Catastrophic Macropinocytosis in Cancer Cells

This PDF file Includes:

Supplementary text

Figures S1 to S11 and Legends

Tables S1 and S2

SI References

SI Materials and Methods

Cell culture and reagents. All human cell lines except Ker-CT and MCF7 were cultured and maintained in DMEM (Hyclone, Logan, UT) cell culture medium supplemented with 10% fetal bovine serum (Sigma, St. louis, MO), 1% of penicillin and streptomycin (Mediatech, Manassas, VA) at 37°C in a 5% CO_2 incubator. Ker-CT were grown in KGM-Gold medium supplemented with BulletKit™ (Lonza 00192060) while MCF7 were cultured in Eagle's Minimum Essential Medium supplemented with 0.01 mg/ml human recombinant insulin and fetal bovine serum to a final concentration of 10%. 4',6-diamidino-2-phenylindole (DAPI) was purchased from Vector Laboratories (Burlingame, CA).

Cell Morphology and viability. Cells were grown in 6-well culture plates and treated with test compounds or vehicle for different duration. A phase contrast microscope (Olympus IX73), were used to capture images to document phenotypic alteration such as ruffling, contraction, rounding, blebbing and bursting. Multiple microphotographs were taken from three independent experiments. Vacuolized cells were counted and presented as percent control. 4-5 randomly chosen fields with 50-100 cells/field for each treatment were evaluated for imaging analysis. Cell viability was determined using 3-(4,5-Dimethylthiazol-2-yl)-2,5-Diphenyltetrazolium Bromide (MTT) dye (St. louis, MO) as described (1). Briefly, 0.5×10^6 RD or RH30 were seeded per well into 6-well culture plates at 37°C in incubator and allowed to attach for 24 h. Next day cells were treated with OSI-027 (0-25 µM, 24 h) or PP242 (0-10 µM, 24 h) and incubated with MTT at final concentration 0.5 mg/ml for 3 h. Formazan crystals were dissolved in DMSO and Optical density was measured at 490 nm. The reduction in viability of cells was expressed as the percentage of control cells.

Transmission Electron Microscopy (TEM). TEM analysis was performed as described (2). Vehicle and OSI-027-treated RD cells were fixed with 2% paraformaldehyde and 2.5% glutaraldehyde in 0.1 M cacodylate buffer. Cells were then placed in an ice-cold solution of 1% osmium tetraoxide (Electron Microscopy Sciences) with 0.8% potassium tetraoxide and 3 mM calcium chloride. Ultrathin sections were prepared and supported on 75 mesh copper grids followed by Sato lead staining. Images were captured in a Tecnai Spirit Twin 20-120 kv electron microscope (FEI, Hillsboro, OR).

Uptake of fluid-phase fluorescent Tracer. Labeling of intracellular vacuoles with fluid-phase tracer was performed as described (3). RMS cells were grown in six well plates. Untreated and OSI-027-treated cells were incubated with LY (1 mg/ml) for 1 h. Alternatively, LY was added at the time of OSI-027 exposure. Cells were washed thrice with PBS and imaged for LY-uptake with an upright fluorescence microscopy (Olympus1X-S8F2, Japan). Cells containing LY only in the vacuoles were counted and presented as percent of vehicle-treated control cells. 30-50 cells from each of 4-6 randomly chosen fields for each treatment were evaluated for quantitative analysis.

Immunofluorescence (IF) staining of cultured cells with antibodies. Cells were grown on either cover slip or chamber slides. Following various treatments, cells were fixed in 4% paraformaldehyde for 10 min, permeabilized with 0.1% Triton X-100 for 15 min. and washed with PBS. After blocking for 1 h with 1% bovine serum albumin, cells were incubated with primary antibodies overnight at 4^0 C, washed three times with PBS, and then incubated with fluorescein-conjugated secondary antibodies for 1 h at room temperature. After three wash with PBS, the slides were mounted with DAPI and examined with a fluorescence microscope (Olympus BX-51 equipped with Olympus DP80 digital camera). In some of the IF experiments, Phalloidin (5 µL/slide, 10-15 min at 37^0C) was employed to detect actin filaments in paraformaldehyde fixed cells before incubating the primary antibodies. List of Primary and secondary antibodies used in this study are listed in *SI Appendix,* Tables S1 and S2. For autophagic fluorescence observation, cells were grown on coverslips and treated with either OSI-027 or Rapamycin. After 24 h, cells were stained with Dansylcadaverine (MDC) (50 µM for 30 min at 37^0C).

siRNA transfection. RMS cells were transfected with siRNAs against human Rictor, Rac1, MAP2K4 or scrambled siRNA purchased from Ambion, Life Technologies (Grand Island, NY). Transfection was carried out using Opti-MEM-I reduced-serum medium (Invitrogen, Grand Island, NY) and lipofectamine 2000 transfection reagent (Sigma, St. Louis, MO) for 24 h.

Immunoblot analysis. Protein quantification and immunoblot analyses were performed as described (4). Cell lysates from various treatment groups were prepared using an ice-cold lysis buffer (Bio-Rad, Hercules, CA). Tissues were homogenized in ice-cold lysis buffer. Protein was quantified using a DC kit (Bio-Rad, Hercules, CA). Lysates were run on to SDS-PAGE and proteins were electrophoretically

transferred to polyvinylidene difluoride (PVDF) membrane. The membranes were blocked with 5% nonfat dry milk and incubated with primary antibodies were probed overnight at 4^0C. Following three washes, the membranes were incubated for 1.5 h with Horseradish peroxidase (HRP)-conjugated secondary antibody. The blots were developed with enhanced chemiluminescence (ECL) according to manufacturer's instructions (Amersham Bioscience). List of primary antibodies used in this study are provided in *SI Appendix*, Table S1.

Tumor xenograft study. Female mice (athymic nu/nu, 3-5 weeks, 20-25 g) used in this study were NCI-strains from Frederick sold by Charles River (Wilmington, MA, USA). All animal procedures followed guidelines and approvals of the Institute Animal Care and Use Committee (IACUC) of the University of Alabama at Birmingham. The control and each treatment groups comprised five animals/group. Cultured RD and RH30 cells were washed, and re-suspended in cold PBS and then were administrated subcutaneously to nude mice in each rear flank (2.5×10^6 RD or RH30 cells/100 µL of cold PBS). Tumor size was measured by digital caliper and tumor volume calculated and plotted as a function of days/weeks post seeding. The durations of the experiments for RD and RH30 xenografts were different as tumors in untreated and treated mice grew at different rates.

In the first experiment (Fig. 6), OSI-027 stock solution was prepared in dimethyl sulfoxide (DMSO) and diluted in corn oil for delivery. Vehicle or OSI-027 (150 mg/kg) was orally administered three time per week starting on day-1 post tumor cells inoculation. Mice body weight and tumor sizes were followed weekly. At the termination of the experiments, mice were sacrificed by CO_2. The subcutaneous tumor was removed, photographed and divided into two pieces. One portion was snap frozen in liquid nitrogen for biochemical analyses. The rest was fixed in 10% buffered formalin and embedded in paraffin. Tissue sections were probed by indirect immunofluorescence analyses for evidence of macropinocytosis, cell death, and EMT.

In the second experiment (Fig. 7), treatment started when the tumors were ~80 mm^3 in size. The mice were treated with vehicle control or OSI-027(75 mg/kg by oral gavage, three time/week), cyclophosphamide (60 mg/kg in PBS by intraperitoneal injection, twice/week), or with both. At the end of the treatment, mice were sacrificed and tumors were excised, fixed in 10% formalin and embedded in paraffin. Tissue sections were examined for histology and by indirect fluorescence probing with antibodies.

Tumor Histology. Tumor tissues were cut into 5 µm. Sections from each group (N=3-5) were deparaffinized in xylene and rehydrated and then stained with hematoxylin and eosin (*H & E*) as described (5). An Olympus BX-51 microscope with Olympus DP80 digital camera was used to capture the images.

Indirect Immunofluorescence (IF) staining of tumor sections. IF was performed as described (5). Briefly, after blocking with buffer of 2.5% bovine serum albumin in PBS for 1 h at 37^0C, the sections were incubated with primary antibodies over night at 4°C. The sections were incubated with fluorescein-conjugated secondary antibodies for 1-2 h at room temperature and rinsed with PBS. Sections were mounted with DAPI. Photomicrographs were captured as described above. List of Primary and secondary antibodies used in this study are listed in *SI Appendix*, Tables S1 and S2.

Terminal deoxynucleotidyl transferase dUTP nick end-labeling assay. TUNEL assay was performed in fixed tissue sections by using the *in situ* DNA fragmentation assay Kit (Roche Diagnostics, Indianapolis, IN) according to the manufacturer's instructions. The sections were then counterstained with DAPI and visualized under a fluorescence microscope for green positive TUNEL signals as just described.

Caspase-3 activity assay. Caspase-3 activity assay was performed as described (6), and quantified at excitation at 380 nm and emission at 440 nm.

Quantitative real time RT-PCR (qRT-PCR). Total RNA isolation and qRT-PCR analyses were performed as described (7). qRT-PCR reactions were carried out in triplicate using 7500 fast Real-Time PCR system (Applied Biosystem, CA, USA). Relative quantification of the steady state target mRNA levels was obtained after normalization of total amount of cDNA to GAPDH endogenous control.

Cellular reactive oxygen species (ROS) detection. ROS cellular localization was determined by fluorescent microscopy using the fluorescent probe DCFDA as described (1). Briefly, 50, 000 cells were plated on coverslip. Next day cells were treated with NAC (5 mM) for 30 min. with or without exposure to OSI-027 for 3 h. The cells were then washed with 1× PBS and subjected to stain with 10 μM DCFDA for 15-20 min. at 37°C. After three PBS washes, the stained cells were imaged with the fluorescence microscope.

Extracellular ATP measurement. RD and RH30 cells were plated onto 96 well flat-bottom plates at a density of 10,000 cells per well and incubated overnight prior with or without to exposure to OSI-027 (10 μM) for 0 to 72 hrs. Then ATP concentrations were measured using a firefly bioluminescence assay kit (ATP Determination Kit A22066, Invitrogen, Waltham, USA) according to supplier's instructions.

Clonogenic survival assay. Clonogenic survival assay was performed as described (4). Briefly, OSI-027 (0-25 μM, 24 h)-treated RD cells were seeded into 6-well plate at cell density of 800-1000 cells per well and were allowed to grow for additional 10 days in humidified chamber at 37^0C with 5% CO_2. Media were replaced on day 5. On day 10, colonies were washed with chilled PBS and fixed with cold methanol, stained with crystal violet, washed and air-dried. Blue colonies were scored and photographed. Data expressed as number of colonies formed relative to the control.

Statistical analysis. Statistical analyses were performed using GraphPad Prism 8. Results were expressed as mean ± standard error of mean (SEM). Statistical analysis between two groups were performed using Student's t test. Multiple treatment groups were analyzed using one-way or two-way analysis of variance (ANOVA). P value of at least 0.05 represents a significant change from their respective groups.

References

1. Srivastava RK*, et al.* (2016) ATF4 regulates arsenic trioxide-mediated NADPH oxidase, ER-mitochondrial crosstalk and apoptosis. *Archives of biochemistry and biophysics* 609:39-50.
2. Darshi M*, et al.* (2011) ChChd3, an inner mitochondrial membrane protein, is essential for maintaining crista integrity and mitochondrial function. *The Journal of biological chemistry* 286(4):2918-2932.
3. Wang JT, Teasdale RD, & Liebl D (2014) Macropinosome quantitation assay. *MethodsX* 1:36-41.
4. Kurundkar D*, et al.* (2013) Vorinostat, an HDAC inhibitor attenuates epidermoid squamous cell carcinoma growth by dampening mTOR signaling pathway in a human xenograft murine model. *Toxicology and applied pharmacology* 266(2):233-244.
5. Srivastava RK*, et al.* (2014) GLI inhibitor GANT-61 diminishes embryonal and alveolar rhabdomyosarcoma growth by inhibiting Shh/AKT-mTOR axis. *Oncotarget* 5(23):12151-12165.
6. Singh R, Pervin S, Wu G, & Chaudhuri G (2001) Activation of caspase-3 activity and apoptosis in MDA-MB-468 cells by N(omega)-hydroxy-L-arginine, an inhibitor of arginase, is not solely dependent on reduction in intracellular polyamines. *Carcinogenesis* 22(11):1863-1869.
7. Kaylani SZ*, et al.* (2013) Rapamycin targeting mTOR and hedgehog signaling pathways blocks human rhabdomyosarcoma growth in xenograft murine model. *Biochemical and biophysical research communications* 435(4):557-561.

SI Tables

Table-S1 List of primary antibodies used in this study.

Antibodies	**Company/Cat No.**	**Application**	**Dilution**	
			For cell culture studies	**For tumor xenograft studies**
EEA1	Cell signaling/ 2411	IF	1:500	1:100
Rab5	Cell signaling/ 3547	IF	1:500	-
LAMP-1	Cell signaling/ 9091	IF	1:500	1:200
p-Raptor (Ser792) (p-mTORC1)	Cell signaling/ 2083	Immunoblot	1:500	-
Raptor (mTORC1)	Cell signaling/ 2280	Immunoblot	1:1000	-
p-Rictor (Thr1135) (p-mTORC2)	Cell signaling/ 3806	Immunoblot	1:500	-
Rictor (mTORC2)	Cell signaling/ 2114	Immunoblot	1:1000	
p-mTOR (Ser2448)	Cell signaling/ 5336	IF	-	1:100
p-AKT (Ser473)	Cell signaling/ 9271	Immunoblot / IF	1:1000	1:100
Akt (pan)	Cell signaling/ 4685	Immunoblot	1:1000	-
p-p70 S6Kinase (Thr389)	Cell signaling/ 9234	Immunoblot	1:1000	-
p70 S6 Kinase	Cell signaling/ 9202	Immunoblot	1:1000	-
p-4E-BP1 (Ser65)	Cell signaling/ 9451	Immunoblot	1:1000	-
p-SEK1/MKK4 (Ser257/Thr261)	Cell signaling/ 9156	Immunoblot	1:1000	-
SEK1/MKK4	Cell signaling/ 9152	Immunoblot	1:1000	-
Snail	Cell signaling/ 3879	Immunoblot	-	1:500
Snail	Abcam/ ab180714	IF	-	1:300
Slug	Cell signaling/ 9585	Immunoblot	-	1:500
Vimentin	Cell signaling/ 5741	IF	-	1:100
E-Cadherin	Abcam/ ab15148	IF	-	1: 100
E-Cadherin	Santa Cruz / sc-8426	Immunoblot	-	1: 500

Twist	Abcam/ ab50887	Immunoblot / IF	-	1:1000/ 1:100
Fibronectin	Abcam/ ab2413	IF	-	1:100
LC3A/B	Cell signaling/ 4108	Immunoblot /IF	1:1000/ 1:500	-
Atg7	Cell signaling/ 8558	Immunoblot	1:1000	-
Beclin-1	Cell signaling/ 3495	Immunoblot	1:1000	-
p-Rac1/cdc42	Cell signaling/ 2461	Immunoblot	1:1000	-
Rac1/2/3	Cell signaling/ 2465	Immunoblot	1:1000	-
Cleaved Caspase-3	Cell signaling/ 9664	Immunoblot / IF	1:1000/ 1:500	1:200
Cyclin D1	Thermo Fisher / MA5-16356	Immunoblot	-	1:5000
PCNA	Cell signaling/ 2586	Immunoblot	-	1:2000
β-actin	Sigma / A5316	Immunoblot	1:3000	1:3000

Table-S2 List of secondary antibodies used in this study.

Antibodies	**Company/Cat No.**	**Application**	**Dilution**
goat anti-rabbit	Pierce	Immunoblot	1:2000
goat anti-mouse	Pierce	Immunoblot	1:2000
mouse anti-goat	Pierce	Immunoblot	1:2000
Alexa Fluor 488 Goat anti-mouse	Invitrogen / A11001	IF	1:300 (for tumor sections) or 1:500 (for cell culture)
Alexa Fluor 594 Goat anti-rabbit	Invitrogen / A11012	IF	1:300 (for tumor sections) or 1:500 (for cell culture)

Alexa Fluor 488 Goat anti-rabbit	Invitrogen / A27034	IF	1:300 (for tumor sections) or 1:500 (for cell culture)
Alexa Fluor 594 Goat anti-mouse	Invitrogen / A11005	IF	1:300 (for tumor sections) or 1:500 (for cell culture)

Fig. S1

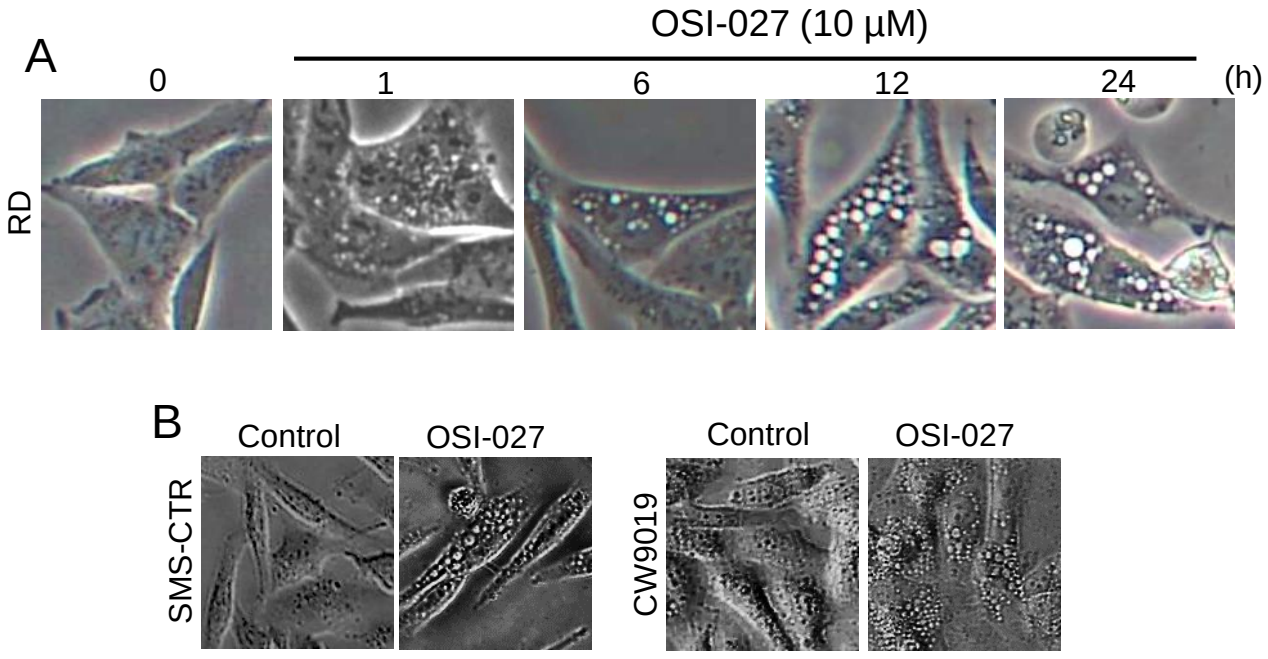

Fig. S1. OSI-027 treatment causes cytoplasmic vacuolization in multiple RMS cancer cells. (*A*) Phase contrast images showing time-dependent effects of OSI-027 (10 μM) on vacuole sizes in RD cells. (*B*) Phase contrast microscopic images showing cytoplasmic vacuolization of OSI-027 (10 μM, 24 h) treatments to SMS-CTR and CW0919 RMS cells. (*C)* Please see separate movie, videography of live RD cells treated with OSI-027 (50 μM, 30 min). The videos were recorded on a phase contrast microscope (Olympus IX73 microscope equipped with Olympus U-LS30-3) to show the development of vacuoles. The recording was done every 3-5 minute for 10 seconds over a period of 30 min. Videos were trimmed, combined and presented on 8X of normal speed.

Fig. S2

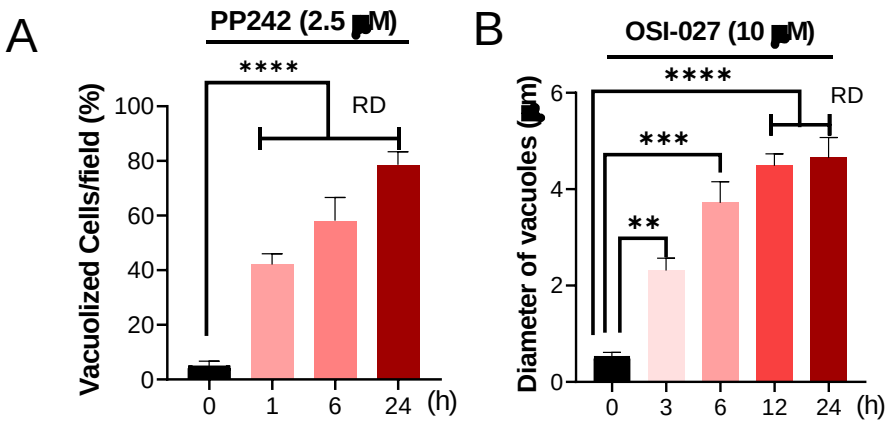
A
PP242 (2.5 μM)
****
RD
Vacuolized Cells/field (%)
100
80
60
40
20
0
0
1
6
24
(h)
B
OSI-027 (10 μM)
****
RD
***
**
Diameter of vacuoles (μm)
6
4
2
0
0
3
6
12
24
(h)

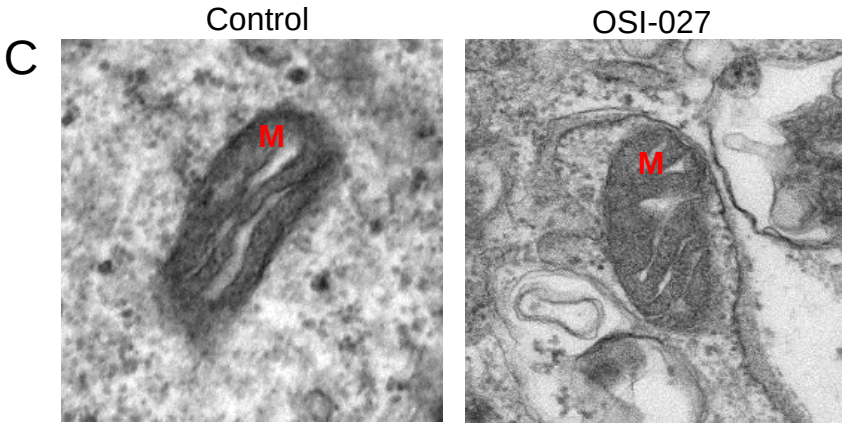
C
Control
OSI-027
M
M

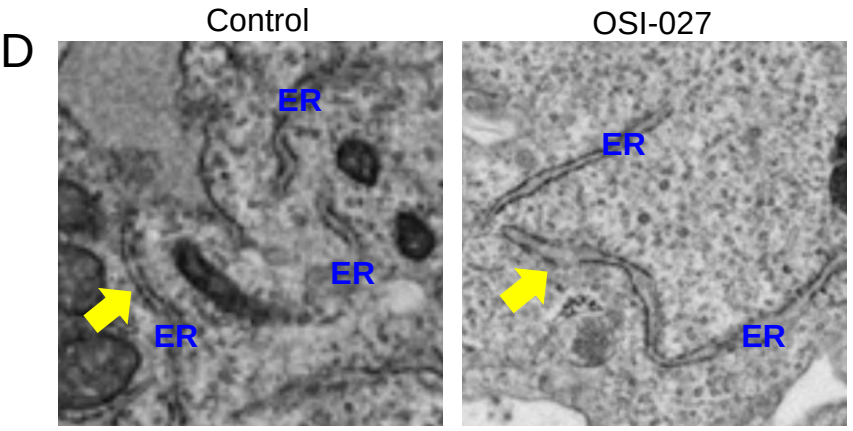
D
Control
OSI-027
ER
ER
ER
ER
ER

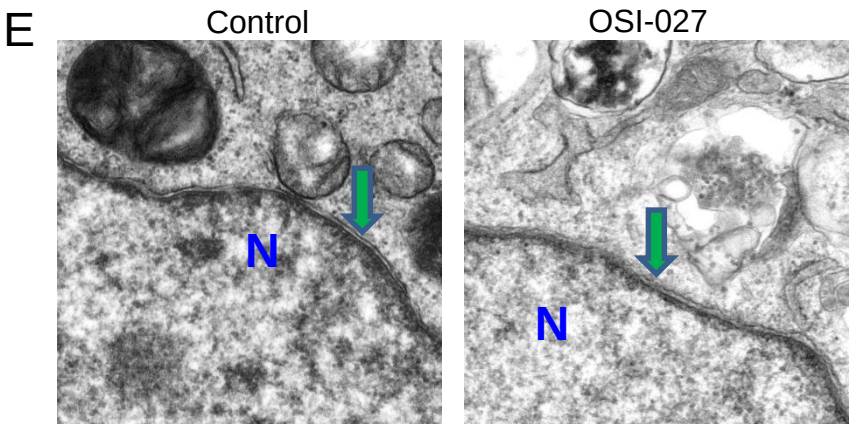
E
Control
OSI-027
N
N

Fig. S2. Transmission Electron Microscopy (TEM) analyses of subcellular organelles in mTORC1/2 inhibitor-treated RD cells. (*A*) Time-dependent effects PP242 (2.5 μM) on the percentages of vacuolized RD cells. (*B)* Time-dependent effects of OSI-027 (10 μM)-induced average vacuole size in RD cells. (*C-E*) TEM images of vehicle (control) and OSI-027-treated RD cells. OSI-027 treatment to RD cells dose not effect (*C*) mitochondrial (denoted by red M) morphology, (*D*) endoplasmic reticulum (ER) (yellow arrows), nor (*E*) nuclear membrane (green arrows). **P<0.01 ***P<0.001, ****P<0.0001 compared to 0 h time-point. These data are representative of three biological replicates.

Fig. S3

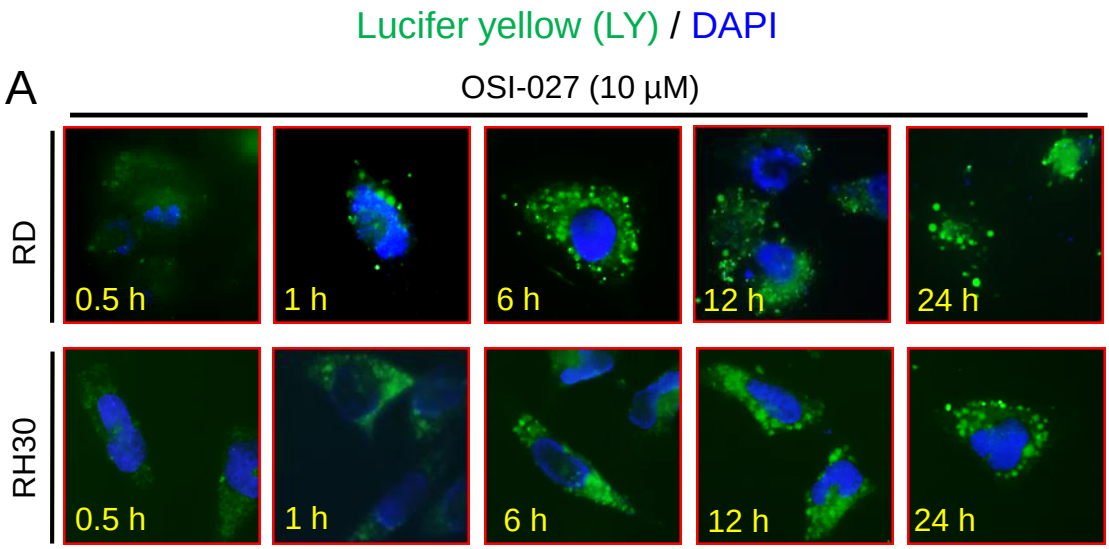
Lucifer yellow (LY) / DAPI
A
OSI-027 (10 μM)
RD
RH30
0.5 h
1 h
6 h
12 h
24 h
0.5 h
1 h
6 h
12 h
24 h

Fig. S3

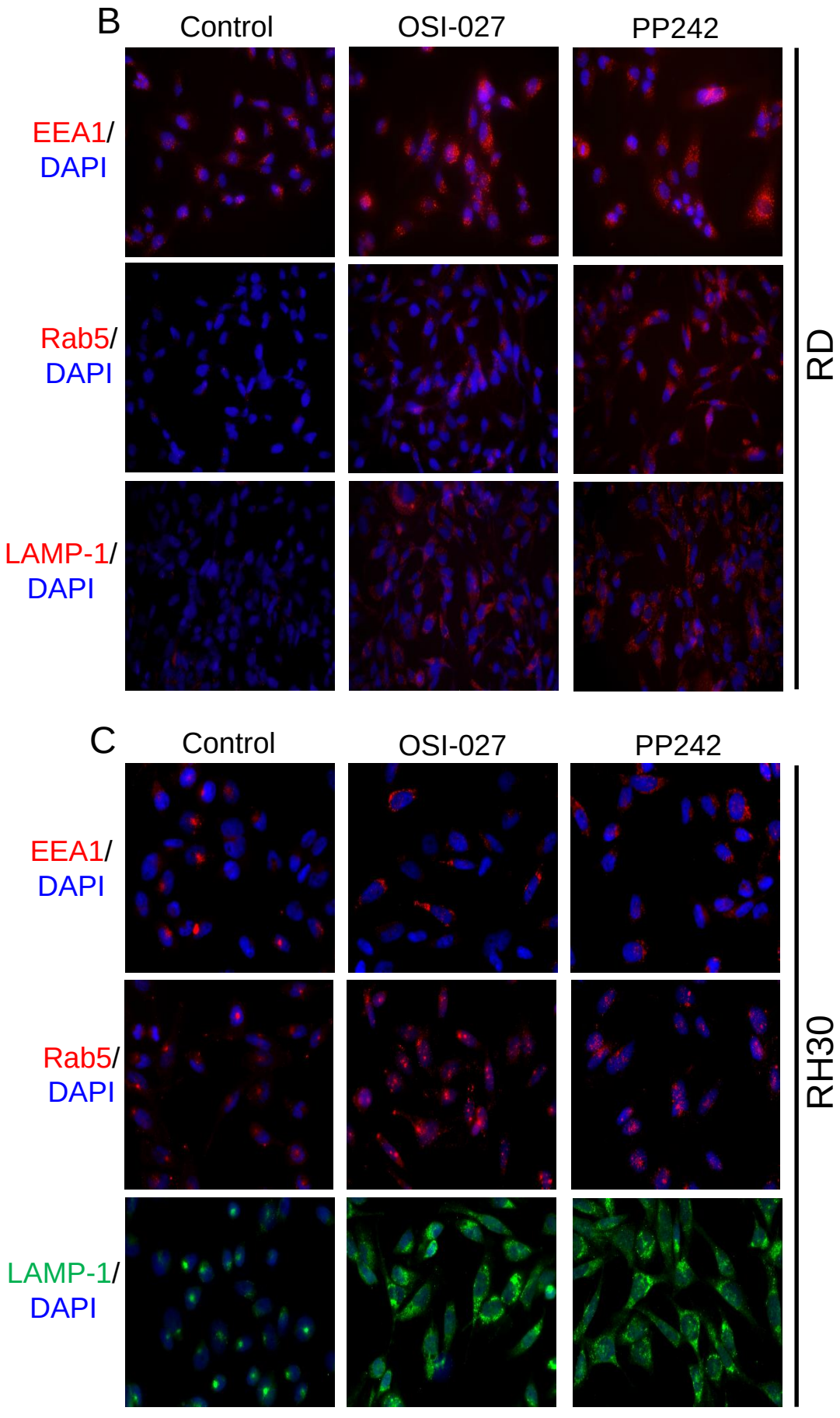
B
Control
OSI-027
PP242
EEA1/
DAPI
Rab5/
DAPI
LAMP-1/
DAPI
RD
C
Control
OSI-027
PP242
EEA1/
DAPI
Rab5/
DAPI
LAMP-1/
DAPI
RH30

Fig. S3

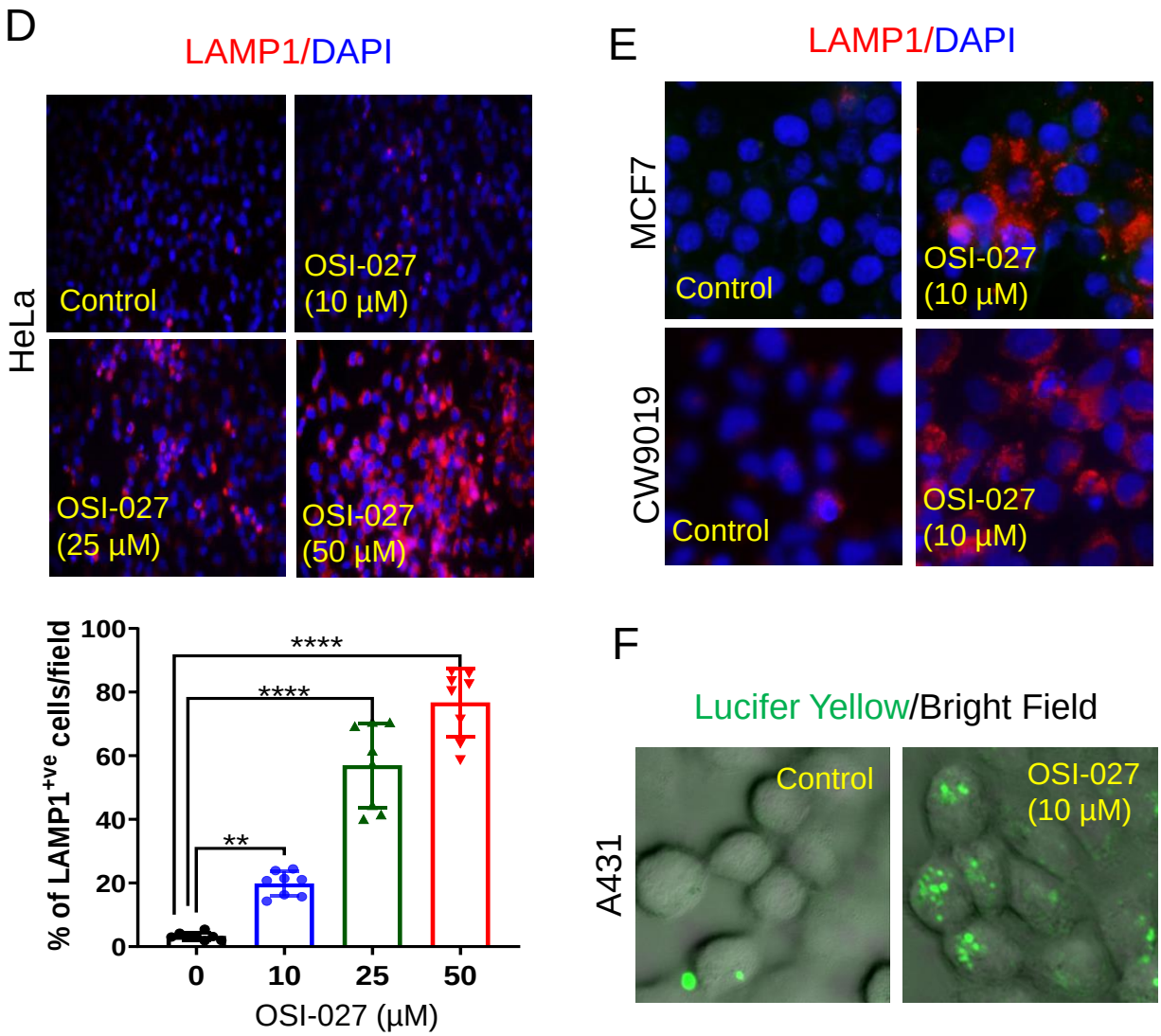

Fig. S3. Characterization of macropinosomes in various cancer cell lines. (*A*) Microphotographs showing LY-accumulation in RD and RH30 cells after exposure to OSI-027 for different duration (0.5 to 24 h). (*B* and *C*) Fluorescence immunostaining for EEA1, Rab5 and LAMP-1 in RD (*B*) or RH30 (*C*) cells treated either with vehicle (control), with OSI-027 (10 µM, 24 h), or PP242 (2.5 µM, 24 h). Cropped images are presented in Fig. 3*C.* (*D*) Dose-dependent effects of OSI-027 on immunofluorescence staining of LAMP-1 in HeLa cells. Histogram showing percentage of OSI-027 (10-50 µM, 24 h) induced LAMP-1 positive cells. (*E*) Immunofluorescence staining of LAMP-1 in OSI-027-treated MCF7 and CW9019 cells. (*F*) Bright field view of Lucifer Yellow uptake in vehicle-treated control or OSI-027 (10 µM, 6 h)-treated A431 cells. **P<0.01, ****P<0.0001 compared to vehicle-treated control. The experiments shown here are representation of three biological replicates.

Fig. S4

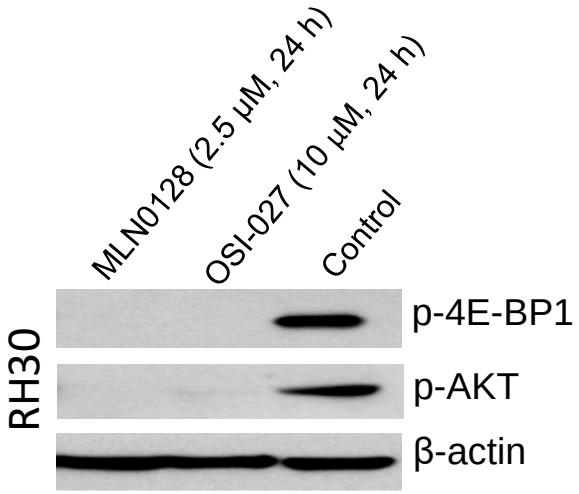

Fig. S4. mTORC1/2 inhibitors block phosphorylation of 4E-BP-1 and AKT in RH30 cells. Immunoblot analyses of RH30 cell lysates treated with MLN0128 or OSI-027 for 24 h.

Fig. S5

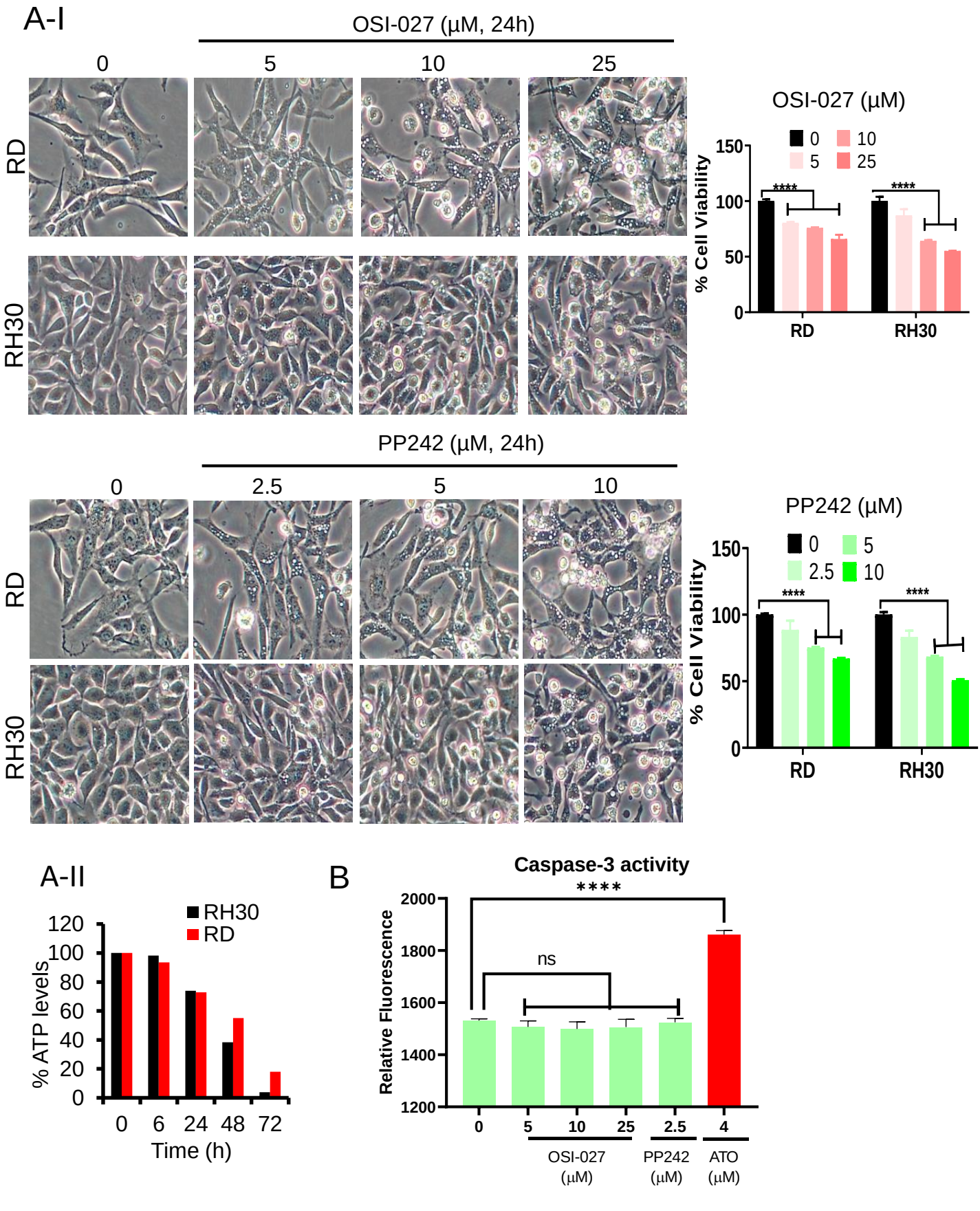
A-I
OSI-027 (μM, 24h)
0
5
10
25
RD
RH30
OSI-027 (μM)
0
5
10
25
% Cell Viability
150
100
50
0
****
****
RD
RH30
PP242 (μM, 24h)
0
2.5
5
10
RD
RH30
PP242 (μM)
0
2.5
5
10
% Cell Viability
150
100
50
0
****
****
RD
RH30
A-II
RH30
RD
% ATP levels
120
100
80
60
40
20
0
0
6
24
48
72
Time (h)
B
Caspase-3 activity
****
ns
Relative Fluorescence
2000
1800
1600
1400
1200
0
5
10
25
2.5
4
OSI-027 (μM)
PP242 (μM)
ATO (μM)

Fig. S5. Dose-dependent effects of OSI-027 on RMS cell death. (*A-I*) Representative microphotographs showing dose-dependent effects of OSI-027 (0-25 µM, 24 h) or PP242 (0-10 µM, 24 h) on % cell viability of RD & RH30 cells. Histograms showing quantification of % cell viability measured by MTT assay. (A-*II*) % ATP levels after OSI-027 (10 µM, 0-72 h) treatment to RD and RH30 cells. (*B*) Histogram showing quantification of caspase-3 activity in vehicle and OSI-027/or PP242-treated RD cells. ATO was used as a positive control. ****P<0.0001 compared to vehicle control. ns- not significant. N=3-6 biological replicates.

Fig. S6

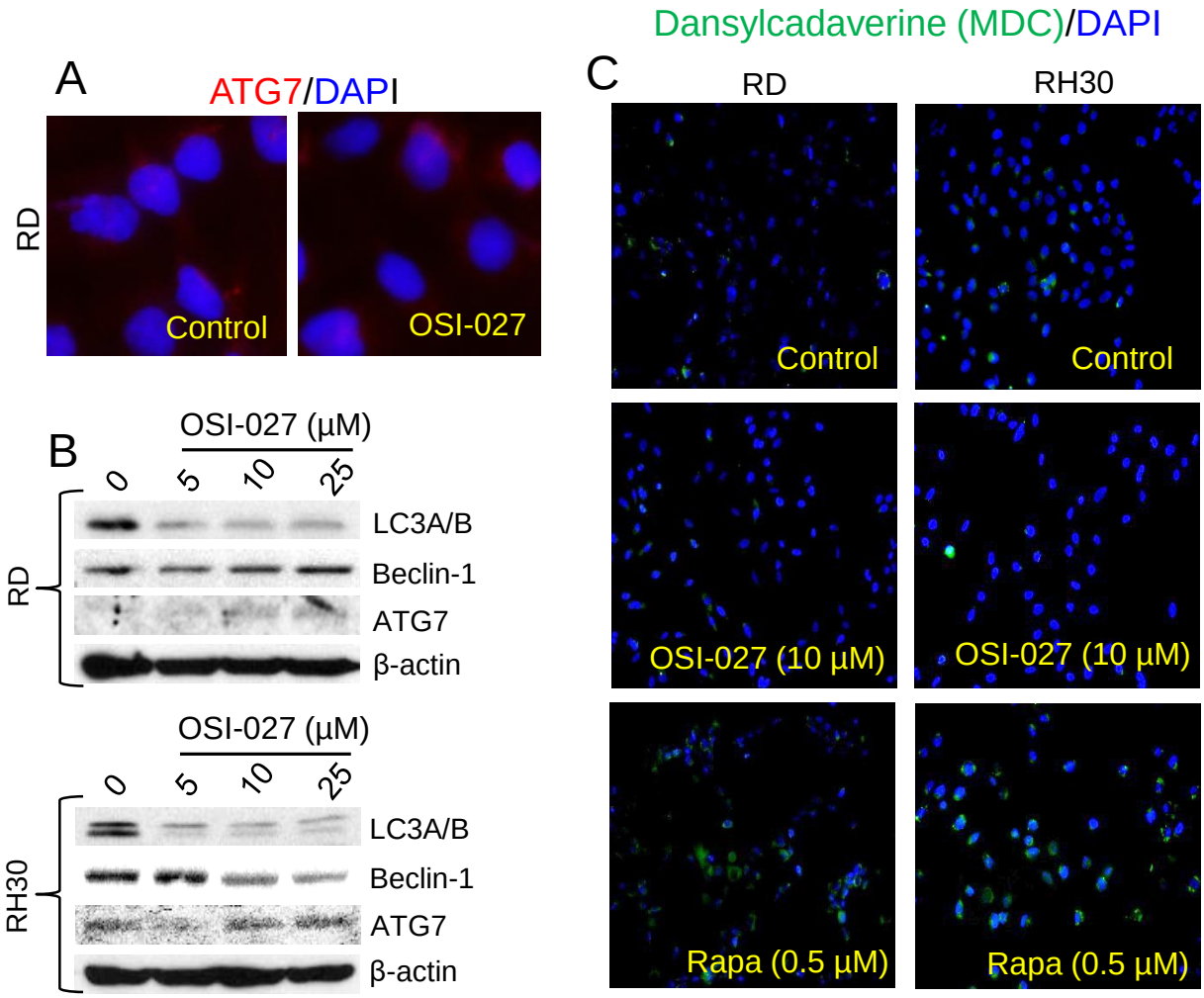

Fig. S6. OSI-027 treatment dose not induce autophagy in RMS cells. (*A*) Immunofluorescence staining of ATG7 in vehicle- (control) and OSI-027 (10 μM, 24 h)-treated RD cells. (*B*) Immunoblot showing dose-dependent effects of OSI-027 (5-25 μM, 24 h) on autophagy regulated proteins, LC3A/B, Beclin-1 and ATG7 in RD and RH30 cells. (*C*) Dansylcadaverine (MDC) staining in vehicle- (control), OSI-027- or rapamycin-treated RD and RH30 cells for 24 h.

Fig. S7

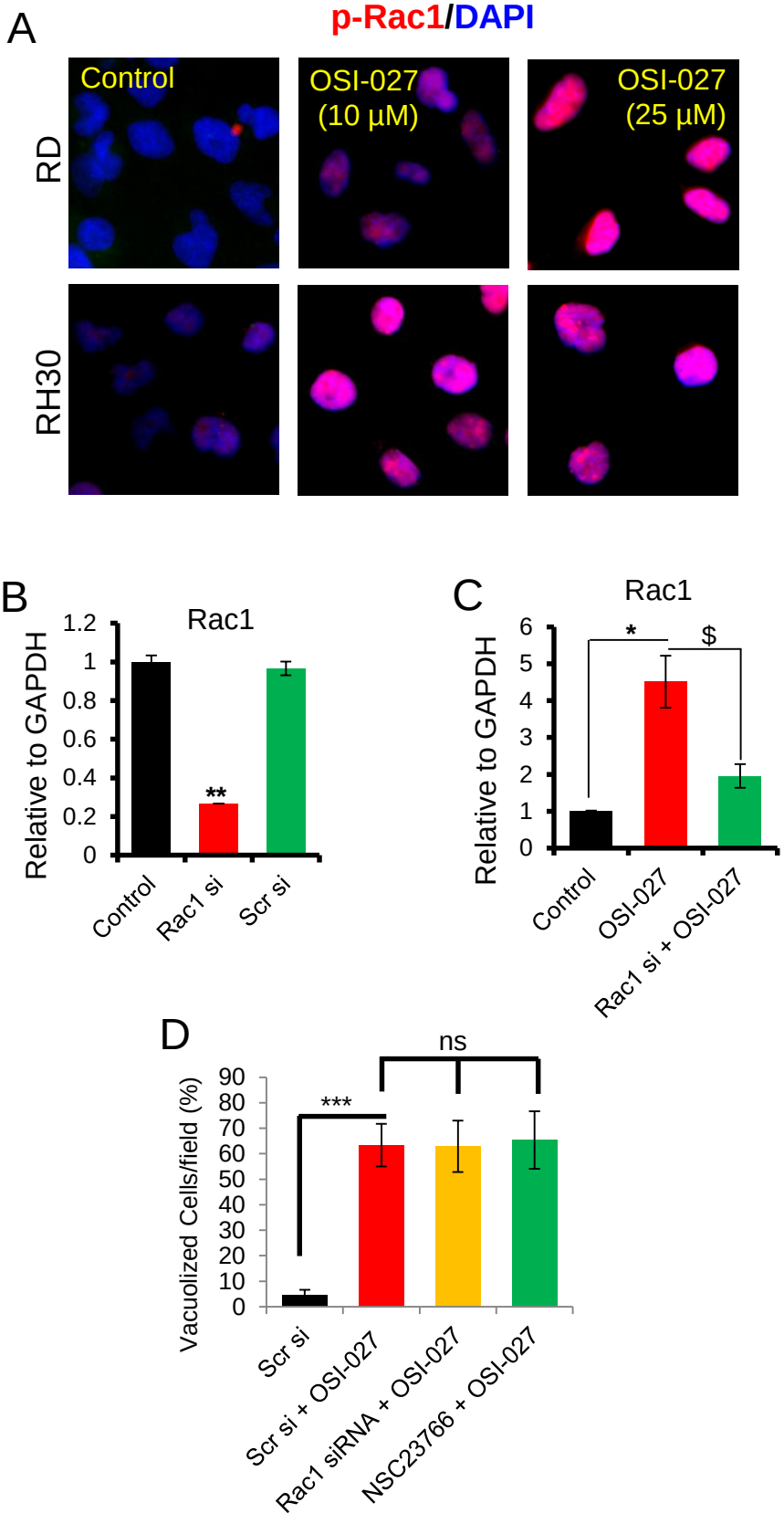
A
p-Rac1/DAPI
Control
OSI-027 (10 μM)
OSI-027 (25 μM)
RD
RH30
B
Rac1
Relative to GAPDH
1.2
1
0.8
0.6
0.4
0.2
0
**
Control
Rac1 si
Scr si
C
Rac1
Relative to GAPDH
6
5
4
3
2
1
0
*
$
Control
OSI-027
Rac1 si + OSI-027
D
Vacuolized Cells/field (%)
90
80
70
60
50
40
30
20
10
0
***
ns
Scr si
Scr si + OSI-027
Rac1 siRNA + OSI-027
NSC23766 + OSI-027

Fig. S7. Rac-1 knockdown dose not alter OSI-027-mediated vacuolization in RMS cells. (*A*) Immunofluorescence staining of p-Rac1 in vehicle- (control) and OSI-027-treated RD and RH30 cells. (*B*) Knockdown efficiency of Rac1 siRNA as measured through real time RT-PCR analysis at 24 h post transfection. (*C*) Real time RT-PCR expression shows the effects of OSI-027 (10 μM and 24 h) and Rac1 siRNA (24 h) on *Rac1* gene expression. (*D*) Histogram showing % quantification of vacuolated RD cells with or without the indicated treatments. *P<0.05, **P<0.01, compared to vehicle-treated control. ***P<0.001 compared to Scr siRNA treatment. $^{\$}$ P<0.05 compared to OSI-027-treated group. ns- not significant between indicated treatment groups.

Fig. S8

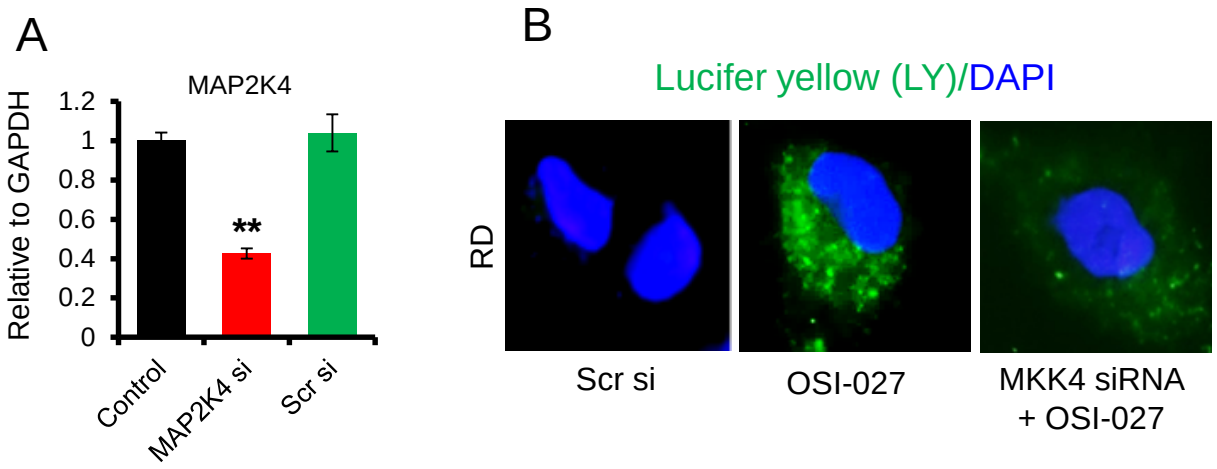

Fig. S8. OSI-027-mediated vacuolization is impaired in MKK4 knockdown RD cells. (*A*) Knockdown efficiency of MAP2K4 siRNA (24 h) as measured through real time PCR analysis. (*B*) LY-accumulation in scrambled control and in MKK4 knockdown RD cells in presence of OSI-027. **P<0.01 compared to vehicle-treated control cells.

Fig. S9

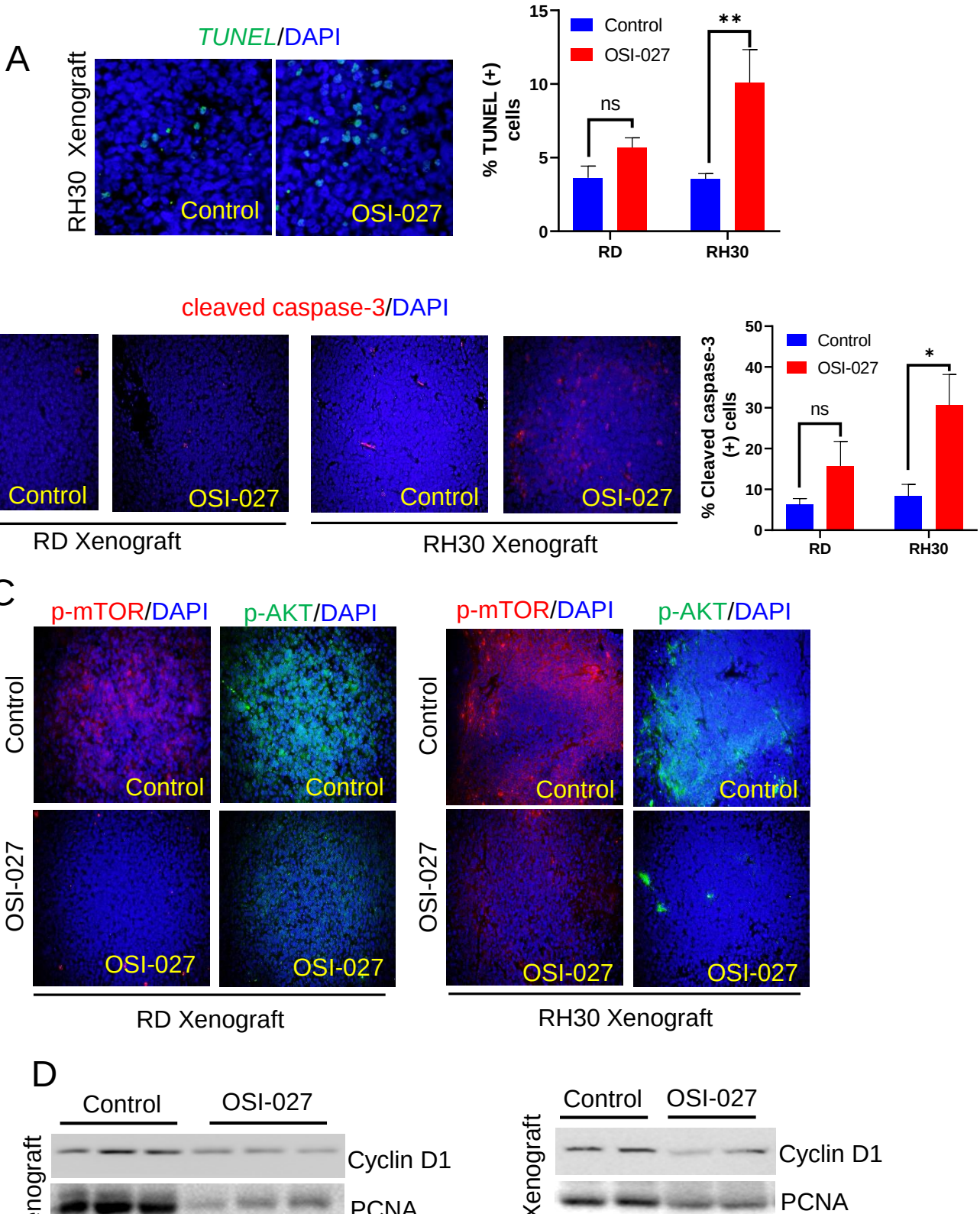
A
TUNEL/DAPI
RH30 Xenograft
Control
OSI-027
% TUNEL (+) cells
Control
OSI-027
ns
**
RD
RH30
B
cleaved caspase-3/DAPI
Control
OSI-027
Control
OSI-027
RD Xenograft
RH30 Xenograft
% Cleaved caspase-3 (+) cells
ns
*
C
p-mTOR/DAPI
p-AKT/DAPI
p-mTOR/DAPI
p-AKT/DAPI
Control
OSI-027
RD Xenograft
RH30 Xenograft
D
Control
OSI-027
RD Xenograft
Cyclin D1
PCNA
β-actin
RH30 Xenograft

Fig. S9. Profile of apoptosis and proliferation biomarkers in OSI-027 treated RMS cells derived xenografts. (*A*) Immunofluorescence staining of green TUNEL-positive cells in the RH30 cells-derived xenograft tumor sections of vehicle- (control) and OSI-027-treated animals. Bar graphs represent % TUNEL-positive cells in the tumor sections of vehicle- and OSI-027-treated RD and RH30 cells derived xenograft. (*B*) Immunofluorescence staining of cleaved caspase-3 in RD & RH30 cells-derived xenograft tumor sections of vehicle- (control) and OSI-027-treated animals. Histograms represent % cleaved caspase-3-positive cells in these the tumor sections. (*C*) Immunofluorescence staining of p-mTOR (Ser2448) and p-AKT (Ser473) in RD & RH30 cells-derived xenograft tumor sections of vehicle- (control) and OSI-027-treated animals. (*D*) Immunoblot analysis of Cyclin D1 and PCNA in tumors lysates obtained from vehicle (control) and OSI-027-treated animals. *P<0.05, **P<0.01 compared to their respective controls. ns- not significant

Fig. S10

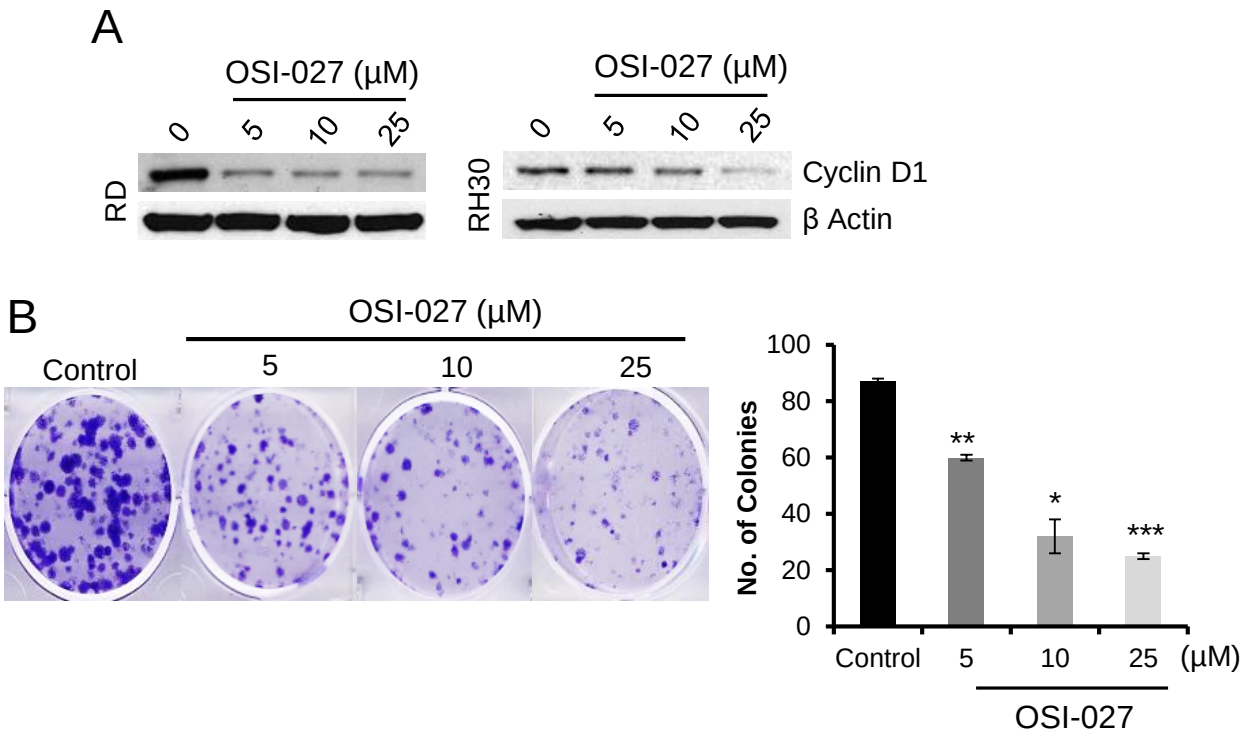

Fig. S10. Effects of OSI-027 on proliferation of RMS cells. (*A*) Reduced cyclin D1 protein expression in OSI-027 (5-25 μM, 24 h) treated cultured RD and RH30 cells. (*B*) Dose-dependent effects of OSI-027 (5-25 μM, 24 h) on RD cell proliferation using colony formation assay. Colonies were stained with crystal violet and photographed. *P<0.05, **P<0.01, ***P<0.001 compared to vehicle-treated control.

Fig. S11

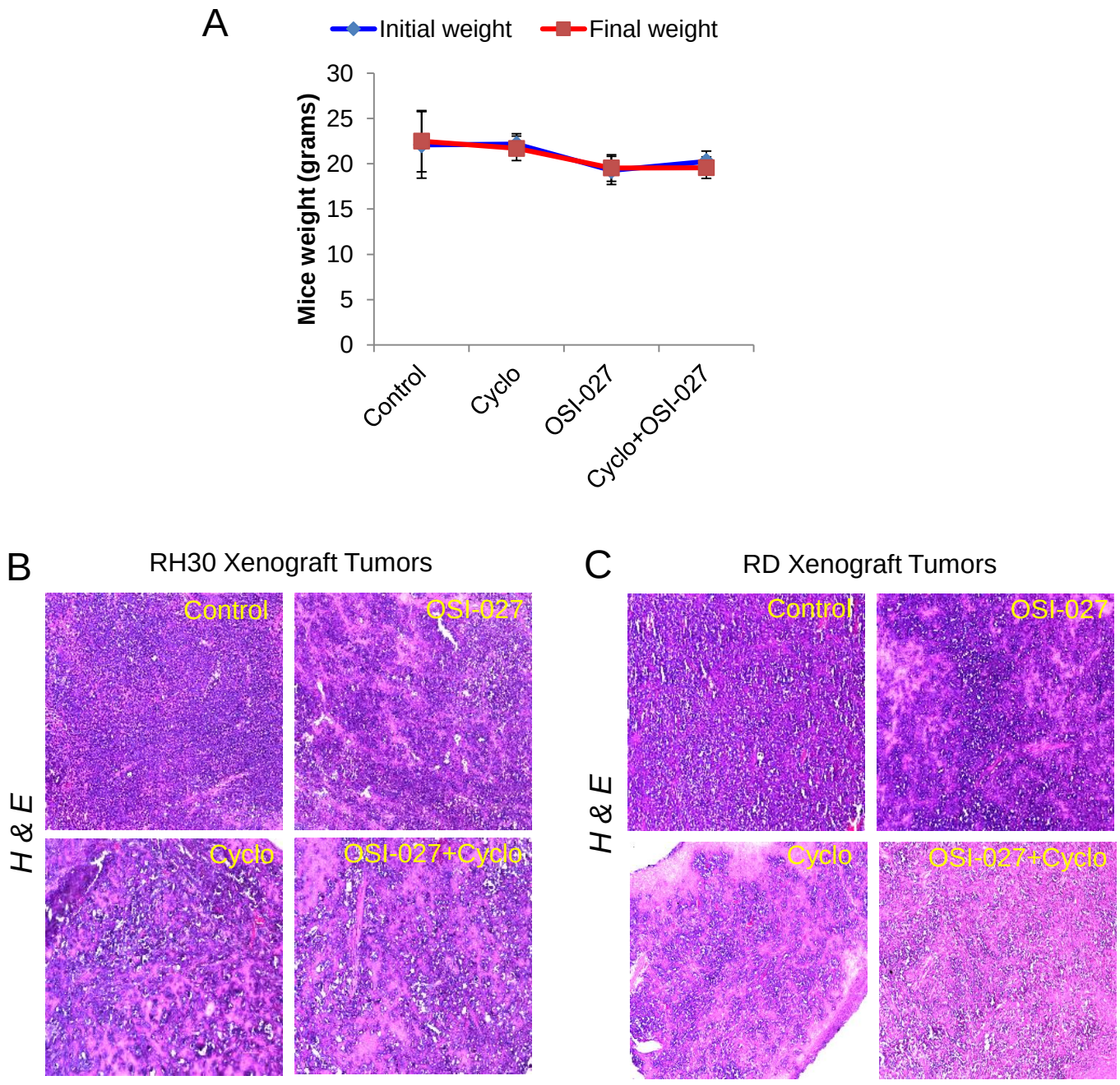

Fig. S11. Body weight of drug treated mice is not significantly altered during the course of treatment. (*A*) Initial and final weights of mice (n=5) following treatment with vehicle, individual drugs, or drug combination. (*B* and *C*) Low magnification images of *H & E* stained sections (5 µm) of formalin fixed xenograft tumors derived from RH30 (*B*) or RD cells (*C*). Cropped images are presented in Fig. 7C.